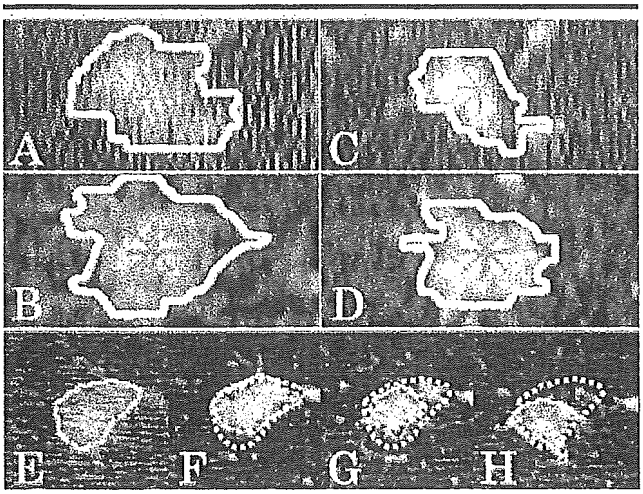

Figure 7. Patient 5. Pulmonary metastasis of adenoid cystic carcinoma. Coronal *(A, C)* and sagittal *(B, D)* images from long-scan-time CT *(A, B)* and thin-section CT *(C, D)* show tumor with extremely irregular contours. (*C* and *D* are approximately in the same plane and at the same level as *A* and *B*, respectively.) Transverse image obtained with long-scan-time CT *(E)* shows contour (outline) of visualized internal target volume. Transverse images obtained with thin-section CT (*F*, at a level 2 mm above that in *E*; *G*, at the same level as *E*; and *H*, at a level 2 mm below *E*) show the target volume with contour lines from *E* (dotted outlines) superimposed for comparison.

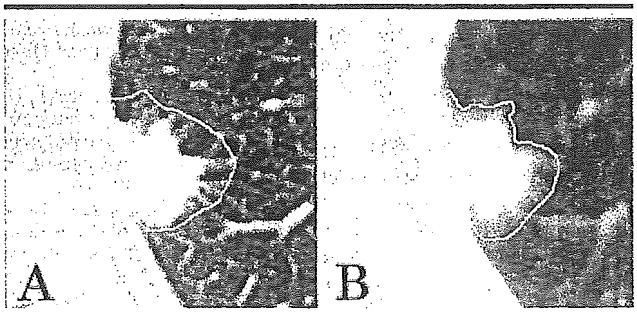

Figure 8. *A*, Transverse thin-section CT image shows tumor with surrounding spiculation that indicates traction-related emphysematous change. *B*, Transverse long-scan-time CT image shows ill-defined margin of tumor with lower attenuation than that on thin-section CT images, a factor that could lead to accidental omission of part of the tumor margin from the target volume. In delineation of tumor margin on long-scan-time CT images, careful reference to tumor features on thin-section CT images is required.

tumor movement during CT was reflected as greater or lesser attenuation because of the partial-volume-averaging effect, depending on the period for which the tumor was in the scanning range during each long-scan-time CT scan. Therefore, we hypothesized that our long-scan-time CT scans reflected the entire trajectory of tumor motion over the course of the respiratory cycle.

To validate this hypothesis, an equation (1) was used to obtain the estimated internal target volume, which was then compared with the visualized internal target volume. Although tumor motion due to breathing is generally greatest in the craniocaudal direction, motion in the left-to-right and anteroposterior directions is also observed (11). To simplify the model, however, we did not factor tumor motion in either the left-to-right or the anteroposterior direction into the equation for estimated internal target volume.

The results of our analysis showed a significantly larger ratio of the visualized internal target volume to the defined gross tumor volume for small tumors than for large tumors. These results indicate that special care must be used in taking internal motion into account when planning treatment of small tumors.

The values for the relative error were within a limited range, except in one case. For tumors that are ovoid and that have an axis of movement that coincides with the craniocaudal direction, our simple model could be applied. Conversely, when the tumor shape was very irregular or when the tumor moved in a different (not craniocaudal) direction, this simple model could not be applied. The shape of the tumor in patient 5, for which a large relative error was found, was so irregular that the simple model of estimated internal target volume could not be applied. The tumor area delineated on long-scan-time CT images was greater than that on corresponding and adjacent thin-section CT images. We surmised that the cause of the unusually large relative error was not the large value of the visualized internal target volume but rather the small value of the estimated internal target volume. We concluded, therefore, that the visualized internal target volume represented a reasonably accurate internal target volume. When we excluded patient 5 from our calculations of relative error, the mean relative error was $-4.1\% \pm 4.1$. The negative value of this result means that the visualized internal target volume was slightly smaller than the estimated internal target volume.

In the case of patient 7, for whom the relative error was an even higher negative value, we failed to delineate an adequate internal target volume on the basis of long-scan-time CT, in that we were not always able to include the fine margin of spiculation that appeared around the nodule on thin-section CT images. We consider this failure to have been caused by the visual merging and resultant obscuration of fine spiculation, consolidation, and emphysematous changes on long-scan-time CT images, whereas these areas were clearly visible on thin-section CT images. The shortcomings of long-scan-time CT therefore must be taken into account, and an area that is wider than the lesion on long-scan-time CT images must be delineated, with reference to thin-section CT images if necessary.

Lagerwaard et al (12) and van Sörnsen de Koste et al (13), on the basis of two helical CT scans and three "slow" CT scans, reported that planning target volumes derived by using slow CT consistently produced superior target coverage than did those from thin-section CT. On the other hand, attempts have been made at some institutions to avoid the influence of respiratory motion during radiation therapy by using active breathing control (14), breath holding (15), and real-time tumor tracking during radiation therapy (16). In some cases, these methods probably are effective for reducing the volume to be irradiated. Although our long-scan-time CT–based planning method might result in a larger target volume than that defined with use of breath control or synchronized irradiation methods, it is simple and can be implemented with a widely available CT scanner and workstation for the planning of radiation therapy.

In this study, one radiation oncologist analyzed the fluoroscopic images and delineated the contours of visualized internal target volumes and of defined gross

tumor volumes. The results of similar analyses performed by multiple clinicians might be inconsistent with our study results because of observer variation.

In addition, many factors, such as the tumor size, shape, and location (upper lobe vs lower lobe) and the pulmonary function, might influence the results of long-scan-time CT. The number of patients (10 patients) used for our analysis was not sufficient to investigate these parameters, and further investigation in a larger patient population is needed to resolve these questions.

In conclusion, the visualized internal target volume and estimated internal target volume were similar in most cases. Long-scan-time CT was capable of depicting virtually the entire trajectory of tumor movement during normal respiration. There were, however, some exceptional cases in which long-scan-time CT images did not accurately depict the internal target volume; therefore, when the tumor margin is delineated on long-scan-time CT images for planning of radiation therapy, thin-section CT images also should be carefully observed for reference.

References

1. Shirato H, Sakamoto T, Takeichi N, et al. Fractionated stereotactic radiotherapy for vestibular schwannoma (VS): comparison between cystic-type and solid-type VS. Int J Radiat Oncol Biol Phys 2000;48:1395–1401.
2. Frighetto L, De Salles AA, Behnke E, Smith ZA, Chute D. Image-guided frameless stereotactic biopsy sampling of parasellar lesions: technical note. J Neurosurg 2003;98:920–925.
3. Uematsu M, Shioda A, Tahara K, et al. Focal, high dose, and fractionated modified stereotactic radiation therapy for lung carcinoma patients: a preliminary experience. Cancer 1998;82:1062–1070.
4. Lax I, Blomgren H, Naslund I, et al. Stereotactic radiotherapy of malignancies in the abdomen: methodological aspects. Acta Oncol 1994;33:677–683.
5. Blomgren H, Lax I, Naslund I, et al. Stereotactic high dose fraction radiation therapy of extracranial tumors using an accelerator. Acta Oncol 1995;34:861–870.
6. Nagata Y, Negoro Y, Aoki Y, et al. Clinical outcomes of 3D conformal hypofractionated single high-dose radiotherapy for one or two lung tumors using a stereotactic body frame. Int J Radiat Oncol Biol Phys 2002;52(4):1041–1046.
7. Uematsu M, Shioda A, Suda A, et al. Computed tomography-guided frameless stereotactic radiotherapy for stage I non-small-cell lung cancer: a 5-year experience. Int J Radiat Oncol Biol Phys 2001;51(3):666–670.
8. Saitoh H, Fujizaki T, Sakai R, Kunieda E. Dose distribution of narrow beam irradiation for small lung tumor. Int J Radiat Oncol Biol Phys 2002;53(5):1380–1387.
9. International Commission on Radiation Units and Measurements (ICRU). Prescribing, recording and reporting photon beam therapy. ICRU Report no. 62 (supplement to ICRU Report no. 50). Bethesda, Md: ICRU, 1999.
10. Balter JM, Ten Haken RK, Lawrence TS, et al. Uncertainties in CT-based radiation therapy treatment planning associated with patient breathing. Int J Radiat Oncol Biol Phys 1996;36:167–174.
11. Seppenwoolde Y, Shirato H, Kitamura K, et al. Precise and real-time measurement of 3D tumor motion in lung due to breathing and heartbeat, measured during radiotherapy. Int J Radiat Oncol Biol Phys 2002;53(4):822–834.
12. Lagerwaard FJ, van Sörnsen de Koste JR, Nijssen-Visser MR, et al. Multiple "slow" CT scans for incorporating lung tumor mobility in radiotherapy planning. Int J Radiat Oncol Biol Phys 2001;51(4):932–937.
13. van Sörnsen de Koste JR, Lagerwaard FJ, Schuchhard-Schipper RH, et al. Dosimetric consequences of tumor mobility in radiotherapy of stage I non-small cell lung cancer: an analysis of data generated using 'slow' CT scans. Radiother Oncol 2001;61:93–99.
14. Wong JW, Sharpe MB, Jaffra DA, et al. The use of active breathing control (ABC) to reduce margin for breathing motion. Int J Radiat Oncol Biol Phys 1999;44(4):911–919.
15. Murphy MJ, Martin D, Whyte R, Hai J, Ozhasoglu C, Le QT. The effectiveness of breath-holding to stabilize lung and pancreas tumors during radiosurgery. Int J Radiat Oncol Biol Phys 2002;53(2):475–482.
16. Shirato H, Shimizu S, Shimizu T, et al. Real-time tumour-tracking radiotherapy. Lancet 1999;353:1331–1332.

Int. J. Radiation Oncology Biol. Phys., Vol. 62, No. 4, pp. 1003–1008, 2005

0360-3016/05/$–see front matter

ELSEVIER

doi:10.1016/j.ijrobp.2004.12.050

CLINICAL INVESTIGATION **Lung**

DIFFERENCES IN PULMONARY FUNCTION BEFORE VS. 1 YEAR AFTER HYPOFRACTIONATED STEREOTACTIC RADIOTHERAPY FOR SMALL PERIPHERAL LUNG TUMORS

TOSHIO OHASHI, M.D.,* ATSUYA TAKEDA, M.D.,*† NAOYUKI SHIGEMATSU, M.D.,* ETSUO KUNIEDA, M.D.,* AKITOSHI ISHIZAKA, M.D.,‡ JUNICHI FUKADA, M.D.,* HOSSAIN M. DELOAR, PH.D.,* OSAMU KAWAGUCHI, M.D.,* TOSHIAKI TAKEDA, M.D.,† KAZUHIKO TAKEMASA, M.D.,† KOUICHI ISOBE, M.D.,§ AND ATSUSHI KUBO, M.D.*

Departments of *Radiology and ‡Internal Medicine, School of Medicine, Keio University, Tokyo, Japan; †Department of Radiology, Tokyo Metropolitan Hiro-o Hospital, Tokyo, Japan; §Department of Radiology, School of Medicine, Chiba University, Chiba, Japan

Purpose: To evaluate long-term pulmonary toxicity of stereotactic radiotherapy (SRT) by pulmonary function tests (PFTs) performed before and after SRT for small peripheral lung tumors.

Methods and Materials: A total of 17 lesions in 15 patients with small peripheral lung tumors, who underwent SRT between February 2000 and April 2003, were included in this study. Twelve patients had primary lung cancer, and 3 patients had metastatic lung cancer. Primary lung cancer was T1–2N0M0 in all cases. Smoking history was assessed by the Brinkman index (number of cigarettes smoked per day multiplied by number of years of smoking). Prescribed radiation doses at the 80% isodose line were 40–60 Gy in 5–8 fractions. PFTs were performed immediately before SRT and 1 year after SRT. Test parameters included total lung capacity (TLC), vital capacity (VC), forced expiratory volume in 1 s (FEV1.0), and diffusing capacity of lung for carbon monoxide (DLCO). PFT changes were evaluated in relation to patient- and treatment-related factors, including age, the Brinkman index, internal target volume, the percentages of lung volume irradiated with >15, 20, 25, and 30 Gy (*V15*, *V20*, *V25*, and *V30*, respectively), and mean lung dose.

Results: There were no significant changes in TLC, VC, or FEV1.0 before vs. after SRT. The mean percent change from baseline in DLCO was significantly increased by 128.2%. Univariate and multivariate analyses revealed a correlation between DLCO and the Brinkman index.

Conclusions: One year after SRT as compared with before SRT, there were no declines in TLC, VC, and FEV1.0. DLCO improved in patients who had been heavy smokers before SRT, suggesting a correlation between DLCO and smoking cessation. SRT seems to be tolerable in view of long-term lung function. © 2005 Elsevier Inc.

Stereotactic radiotherapy, Lung tumors, Pulmonary function.

INTRODUCTION

Stereotactic radiotherapy (SRT) has been shown to be highly effective for treating small and well-circumscribed brain metastases, regardless of the primary site or histology (1, 2). This suggests that small, well-circumscribed extracranial malignancies may be controlled with similar focal, high-dose radiation therapy (3). Uematsu *et al.* have performed CT-guided, small-volume hypofractionated radiotherapy, giving 50–60 Gy in 5–10 fractions, with excellent results (3, 4). They reported a 3-year overall survival rate of 66% for all 50 patients with Stage I non–small-cell lung carcinoma, and of 86% for 29 medically operable patients, suggesting the effectiveness of image-guided, small-volume radiotherapy for lung tumors (4).

We previously reported the serial radiologic changes of the pulmonary opacities after hypofractionated SRT on CT scans (5). Out of 22 lesions, ground-glass opacities were observed in 4 (18%) cases, and dense consolidation developed in 16 (73%).

However, there have been few published reports assessing impaired pulmonary function qualitatively by comparing values obtained before and after hypofractionated SRT (6). In this study, we determined changes in pulmonary function associated with hypofractionated SRT for small peripheral lung tumors to assess the safety of hypofractionated SRT in terms of long-term pulmonary function.

Reprint requests to: Naoyuki Shigematsu, M.D., Department of Radiology, School of Medicine, Keio University, 35 Shinanomachi, Shinjuku-ku, Tokyo 160-8582, Japan. Tel: (+81) 3-5363-3835; Fax: (+81) 3-3359-7425; E-mail: shige@rad.med.keio.ac.jp

This work was partly supported by a grant from Tokyo Ri-Igaku Kenkyujo, Japan.

Received Sep 23, 2004, and in revised form Dec 9, 2004. Accepted for publication Dec 17, 2004.

PATIENTS AND METHODS

Patient and tumor characteristics

Between February 2000 and April 2003, we performed SRT for a total of 17 lesions in 15 patients (14 men and 1 woman) with small-volume lung tumors, whose ages ranged from 57 to 89 years with a median age of 77 years, at the Tokyo Metropolitan Hiro-o General Hospital (Table 1). Twelve patients had primary lung cancer, and other patients had metastatic lung cancers. All 12 patients with primary lung cancer had histologically diagnosed non–small-cell lung carcinoma (adenocarcinoma, $n = 9$; squamous cell carcinoma, $n = 2$; undifferentiated carcinoma, $n = 1$) and were clinically staged as T1–2N0M0. Among the 5 lesions in the 3 patients with metastatic lung cancer, 2 were adenocarcinomas (originating from colonic cancer in 2 patients), and 3 were squamous cell carcinomas (originating from oropharyngeal cancer in 1 patient). For most patients, surgery was not indicated, because of patient age, multiple lesions, or poor pulmonary function. Two patients refused surgery despite having operable tumors. Five patients had chronic obstructive pulmonary disease. One patient had undergone pulmonary lobectomy.

Smoking history was expressed using the Brinkman index, as calculated by multiplying the number of cigarettes per day by the years of smoking, and ranged from 0 to 2640 (median, 875). None of the smokers resumed smoking after SRT. SRT was generally considered if the tumor was 4 cm or smaller in diameter, if craniocaudal breathing-associated motion of the lesion was 1 cm or less, if 3 or fewer lesions were present at the start of treatment, and if all lesions except pulmonary lesions were controlled. SRT and lung function examinations were approved by the institutional review board at each institution. Written informed consent was obtained from each patient before SRT.

Treatment

The planned target volume was determined using CT (Xvision, Toshiba) performed on patients who were breathing at rest. Serial 2-mm-thick scans were obtained in 2-mm increments at 8 s per slice (120 kVp, 200 mAs). Longer scanning periods were used to define the tumor trajectory associated with respiratory and other movements; i.e., the internal target volume (ITV) can be visualized (6). Planning target volume (PTV) was determined from the ITV, with setup margins of 8 mm in all directions.

Table 1. Patients, tumors, and treatment characteristics

Characteristics		Median
Age (year)	57–89	77
Gender		
Male	14	
Female	1	
Tumor		
Primary	12	
Metastatic	5	
Pathology		
Adenocarcinoma	11	
Squamous cell carcinoma	5	
Undifferentiated carcinoma	1	
Internal target volume (cm^3)	3–31	11
Planning target volume (cm^3)	20–86	38.2
Prescribed dose (Gy)	40–60	50
V15 (%)	4.0–18.0	8
V20 (%)	2.0–12.0	7
V25 (%)	2.0–10.0	5
V30 (%)	1.0–8.0	5
Mean lung dose (Gy)	2.25–8.95	4.12

Abbreviation: Vx = the percentage of lung volume irradiated with $>x$ Gy.

Target volumes were calculated according to the following formulas:

$$ITV = 4/3\pi \times R1 \times R2 \times R3 \quad (1)$$

$$PTV = 4/3\pi \times (R1 + 8\text{ mm}) \times (R2 + 8\text{mm}) \times (R3 + 8\text{ mm}) \quad (2)$$

where *R1* (half the maximum diameter), *R2* (half the diameter perpendicular to *R1*), and *R3* (half the maximum diameter in the craniocaudal direction) were obtained with calipers on CT. The diameter in the craniocaudal direction was defined as the product of the thickness and the number of slices from the top to the bottom of the lesion (6).

A radiation treatment planning system (FOCUS version 2.7.0., Computerized Medical Systems, Inc.; St. Louis, MO) was used. We set the treated volume so as to include the PTV within an 80% isodose of the maximum dose, and the 80% isodose was defined as the therapeutic dose. The multileaf collimator moved dynamically according to the tumor shape to irradiate the tumor from 8 different arcs.

In general, radiation doses of 50 Gy were delivered in 5 fractions over 5 to 7 days. Two patients also received conventional radiation therapy (30–40 Gy given in 15–20 fractions over 2–4 weeks) before SRT. No patients received chemotherapy or surgery within 1 year after SRT. The dose–volume histograms (DVHs) were analyzed: *V15*, *V20*, *V25*, and *V30* (the percentages of lung volume irradiated with >15, 20, 25, and 30 Gy, respectively), and mean lung dose (MLD) was obtained for each patient.

Pulmonary function tests

Typical pulmonary function tests (PFTs) were performed before SRT and approximately 1 year after SRT. Test parameters included total lung capacity (TLC), vital capacity (VC), forced expiratory volume in 1 s (FEV1.0), and diffusing capacity of lung for carbon monoxide (DLCO). The results obtained 1 year after SRT were compared with those before SRT.

Pulmonary symptoms

Patients were interviewed monthly for pulmonary symptoms, including dyspnea on exertion and shortness of breath, and the need for steroids and oxygen treatment. Simultaneously, transdermal oxygen saturation was measured. Toxicity was recorded based on the National Cancer Institute Common Toxicity Criteria, version 2.0 (7).

Statistical analysis

We analyzed factors correlating with PFT changes before vs. after SRT.

The Wilcoxon test was used to compare pulmonary function values obtained before and after SRT. Univariate analyses were performed to assess patient- and treatment- related factors, including age, smoking history (Brinkman index), ITV volume, *V15*, *V20*, *V25*, *V30*, and MLD. Multivariate analyses of the same factors were performed using the logistic regression test. Analyses were carried out using SPSS 12 (SPSS Inc., Chicago, IL). Statistical analysis was regarded as statistically significant at p value less than 0.05.

RESULTS

Lung dose and tumor response

The ITV volume, the PTV volume, *V15*, *V20*, *V25*, *V30*, and MLD are listed in Table 1.

Local control was achieved in 16 lesions (94.1%), whereas 1 lesion recurred. The patient with the recurrent lesion had no decline in pulmonary function. Lesions metastasized to other lung sites in 2 of the 15 patients (13.3%), but pulmonary function did not decrease in either patient. All are still alive, to date.

Pulmonary function tests

The results of PFTs before and after SRT are listed in Table 2. The median TLC after SRT was 96.0% of the baseline ($p = 0.08$) (Fig. 1). The median VC after SRT was 97.3% of the baseline ($p = 0.29$) (Fig. 2). The median FEV1.0 after SRT was 99.7% of the baseline ($p = 0.39$) (Fig. 3). The median percent change in DLCO from baseline was 128.2% after SRT; i.e., median DLCO increased significantly from 13.65 mL/min/mmHg before SRT to 17.85 mL/min/mmHg after SRT ($p = 0.039$) (Fig. 4).

Clinical symptoms

Thirteen patients had no respiratory symptoms of more than Grade 2. No narcotic antitussives or steroids were used. One patient experienced a temporary worsening of clinical symptoms, i.e., dyspnea and cough requiring antitussives on exertion. In 1 of the 2 patients treated with external irradiation followed by SRT, pneumonitis in the irradiation field corresponded to clinical manifestations, and steroids were prescribed. Oxygen saturation was 96%–99% before and after SRT in all patients, thus ruling out a decrease in oxygen saturation associated with SRT.

Statistical analysis

We performed univariate analyses for treatment-related factors to assess the mean percentage changes from baseline in PFT parameters. No factors were significantly related to mean changes in TLC, VC, and FEV1.0. On the contrary, there was a statistically significant positive correlation between mean percent changes in DLCO and the Brinkman index ($p = 0.013$, $r = 0.644$; Fig. 5). No other factors were significantly related to DLCO. According to multivariate analysis of the same factors using logistic regression analysis, only Brinkman index was significant ($p = 0.045$).

Changes in DLCO before vs. after SRT were analyzed in 2 clusters: 1 in which the Brinkman index was equal to or less than 400 and the other in which the index exceeded 400 (Fig. 6). Although changes in DLCO were not significant in the group with a Brinkman index ≤400, an elevation of DLCO was noted in the group with a Brinkman index >400.

DISCUSSION

Comparison with surgery

There are a large number of reports comparing pulmonary functions before and after surgery for peripheral lung cancer. Takizawa *et al.* reported postoperative pulmonary function in 40 patients undergoing segmentectomy and another 40 receiving lobectomy for peripheral lung cancer 2 cm or less in diameter. The mean percent changes in forced vital capacity and FEV1.0 from baseline 1 year after surgery were 94.9% and 93.3%, respectively, in the segmentectomy group and 91.0% ($p = 0.14$) and 87.3% ($p = 0.03$), respectively, in the lobectomy group (8).

Bolliger *et al.* compared pre- and postoperative pulmonary functions in 50 patients who underwent lobectomy and 18 who underwent pneumonectomy (9). They found that forced vital capacity, FEV1.0, and TLC decreased by 7%, 9%, and 10% in the lobectomy and by 36%, 34%, and 33% in the pneumonectomy group, respectively.

Kaseda *et al.* compared pre- and postoperative lung function and 5-year survival in 44 patients undergoing video-assisted thoracic surgery lobectomy (VATS) and 77 undergoing open thoracotomy. Percent changes from baseline (before operation) in postoperative VC and FEV1.0 were 84.9% and 84.8% in the VATS group and 66.8% and 71.2% in the open thoracotomy group ($p < 0.0001$ for both),

Table 2. Results of pulmonary function tests before and after stereotactic radiotherapy

	Before SRT		After SRT		
	Range	Median	Range	Median	p value
TLC (mL)	3,990–7,180	5,520	3,630–7,420	5,295	0.08
VC (mL)	2,360–4,990	2,870	2,220–5,080	2,740	0.29
FEV1.0 (mL)	850–3,800	1,990	860–3,600	1,800	0.39
DLCO (mL/min/mmHg)	7.4–29.4	13.65	9.69–28.9	17.85	0.039

Abbreviations: DLCO = diffusion capacity of the lung for carbon monoxide; FEV1.0 = forced expiratory volume in one second; SRT = stereotactic radiotherapy; TLC = total lung capacity; VC = vital capacity.

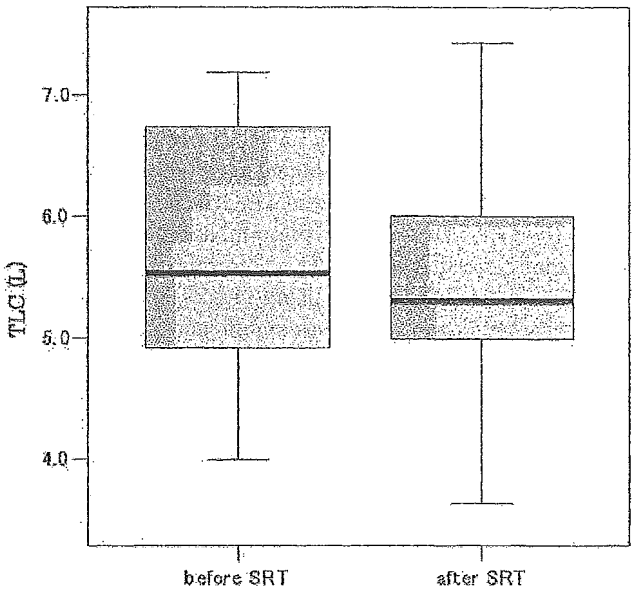

Fig. 1. Change in total lung capacity (TLC). There was no statistically significant difference in TLC before stereotactic radiotherapy (SRT) vs. 1 year after SRT ($p = 0.08$). The lowest and highest 10% of the data are shown as points beyond the error bars. The box includes the central 50% of the data (25–75%). The solid line within each box is the median of the data.

respectively. The 5-year survival rate was significantly higher in the VATS group (97.0%) than in the open thoracotomy group (78.5%) ($p = 0.0173$) (10).

Because surgery for lung carcinoma is associated with removal of both air passages and parenchymal lung tissue, FEV1.0 can diminish, as evidenced by lung perfusion scans and predicted by the following formula: *postoperative FEV1.0 = preoperative FEV1.0 × percent perfusion of*

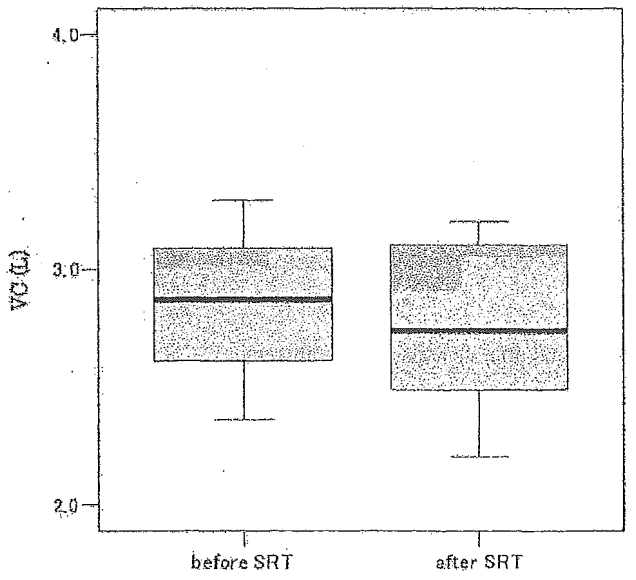

Fig. 2. Change in vital capacity (VC). There was no statistically significant difference in VC before stereotactic radiotherapy (SRT) vs. 1 year after SRT ($p = 0.29$).

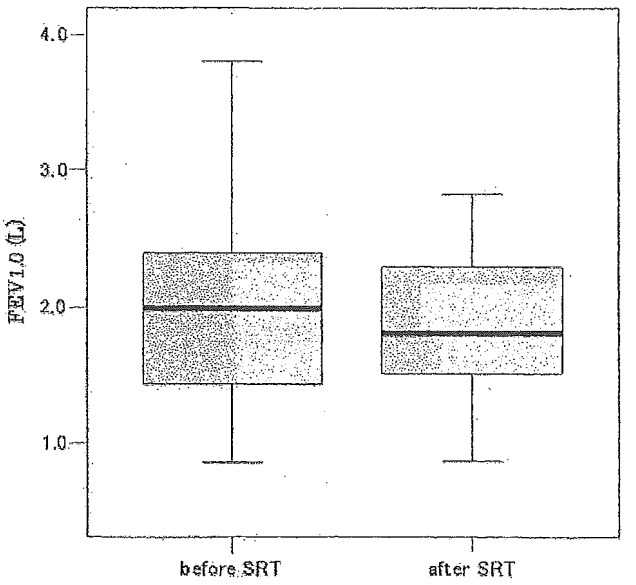

Fig. 3. Change in forced expiratory volume in 1 s (FEV1.0). There was no statistically significant difference in FEV1.0 before stereotactic radiotherapy (SRT) vs. 1 year after SRT ($p = 0.39$).

remaining lung (11). When patients are predicted to have FEV1.0 of 800–1000 mL after surgery, they are not generally considered to be appropriate candidates for surgery (12). In this study, even a pre-SRT FEV1.0 of less than 1000 mL was not associated with a post-SRT decline in FEV1.0, indicating that SRT is feasible even for inoperable patients, because of their decreased pulmonary function.

Comparison with conventional radiotherapy

Some authors have reported the results of pulmonary function tests after conventional radiotherapy for lung can-

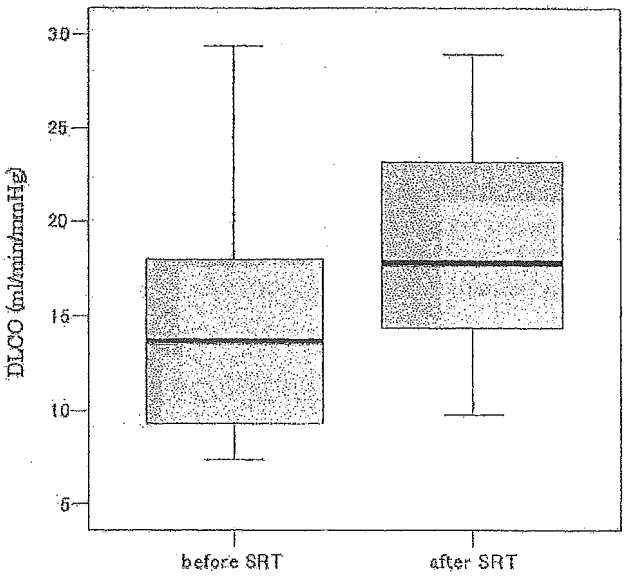

Fig. 4. Change in diffusion capacity of the lung for carbon monoxide (DLCO). There was a statistically significant difference in DLCO before stereotactic radiotherapy (SRT) vs. 1 year after SRT ($p = 0.039$).

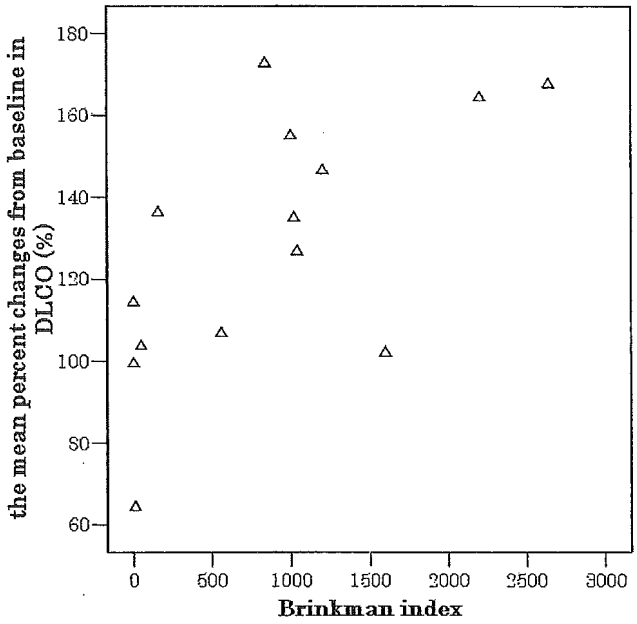

Fig. 5. Scatter plot of the Brinkman index (calculated by multiplying cigarettes per day and years of smoking) vs. the mean percent changes from baseline in diffusion capacity of the lung for carbon monoxide (DLCO).

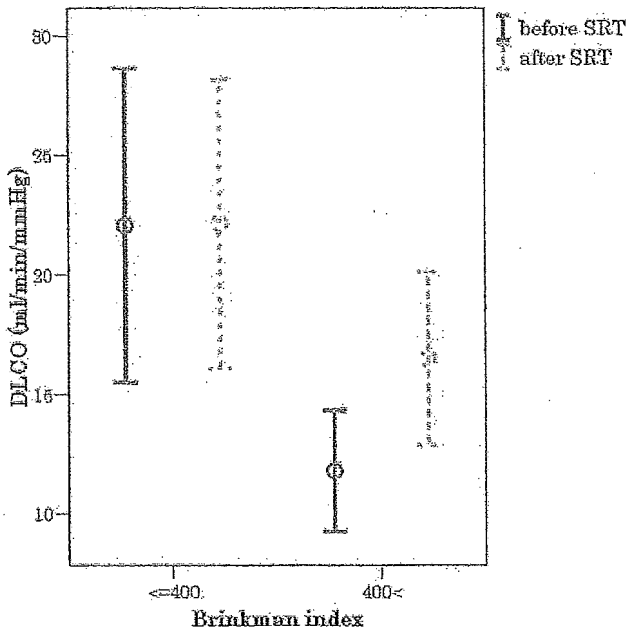

Fig. 6. Comparison of diffusion capacity of the lung for carbon monoxide (DLCO) before vs. after stereotactic radiotherapy (SRT) between the group with a Brinkman index ≤400 and the group with a Brinkman index >400.

cer (13, 14). Sunyach *et al.* reported that three-dimensional conformal radiotherapy for non–small-cell lung carcinoma (Stage I in 8 patients, Stage II in 13 patients, Stage IIIA in 17 patients, and Stage IIIB in 16 patients) significantly decreased TLC by 6.5% as compared with the predicted value, but there was no significant change in DLCO or FEV1.0 (14). In another study, Abratt and Wilcox reported that a conventional anteroposterior parallel-opposed field significantly decreased DLCO, by 14%, and that TLC had decreased by 7% at 6 months (15).

To our knowledge, there are no reports concerning changes in pulmonary function associated with conventional radiotherapy in patients with early lung cancer. Onimaru *et al.* reported changes in pulmonary function immediately after image-guided radiotherapy (IGRT) for non–small-cell lung carcinoma. They performed IGRT in 46 patients with lung cancers 0.6–6 cm in diameter and measured VC before and after IGRT in 9 patients and FEV1.0 and DLCO in 8 of the 9. These authors found no significant changes in VC, FEV1.0, or DLCO (5). Our study showed percent changes from baseline to be 96.8% for VC and 99.3% for FEV1.0; i.e., symptoms did not worsen after SRT. Our findings are more favorable than those obtained with surgical procedures, including lobectomy, segmentectomy, and VATS. Furthermore, our results are also better than those obtained with conventional radiotherapy.

Although the results for both VC and FEV1.0 in our study were equivalent to those in the study of Onimaru *et al.* (5), DLCO improved after SRT in our patients, with the percent change from pretreatment DLCO being 128%. There was a significant correlation between the improvement in DLCO and the Brinkman index; i.e., although no changes in DLCO were observed in the group with a Brinkman index ≤400, DLCO markedly improved in the pre-SRT heavy smokers (Brinkman index >400). Sansores *et al.* reported a significant increase in DLCO 1 week after smoking cessation, but no further increase was noted 1 or 3 months later (16). Because complete post-SRT smoking cessation was documented in our facilities, we speculate that smoking cessation may be more beneficial in terms of improving DLCO than SRT.

Graham *et al.* analyzed 99 cases of non–small-cell lung cancer and found *V20* to correlate well with the incidence of symptomatic pneumonitis. Furthermore, values of *V20* less than 25%, 25%–37%, and more than 37% were associated with estimated radiation pneumonitis incidences of 0–4%, 2–12%, and 19–30%, respectively (17). Tsujino *et al.* suggested that the *V20* can serve as a predictor of radiation pneumonitis after concurrent chemoradiation for lung cancer (18). In the present study, none of our patients who had *V20* of less than 25% developed symptomatic radiation pneumonitis. However, further study is required to determine whether the results of Graham *et al.* are applicable, because there are differences in single radiation doses, the number of irradiations, and the duration of the entire treatment between conventional radiation therapy and SRT (17).

CONCLUSIONS

Lung function testing, performed before and after SRT for small peripheral lung tumors, showed decreases in VC

and FEV1.0 to be less than those after surgical procedures, including lobectomy, segmentectomy, and VATS. However, the DLCO improvement in this study requires further investigation. In terms of long-term pulmonary function, SRT seems to be feasible and applicable to patients with poor lung functions.

REFERENCES

1. Alexander E III, Moriarty TM, Davis RB, *et al.* Stereotactic radiosurgery for the definitive, noninvasive treatment of brain metastases. *J Natl Cancer Inst* 1995;87:34–40.
2. Flickinger JC, Kondoziolka D, Lunsford LD, *et al.* A multi-institutional experience with stereotactic radiosurgery for solitary brain metastasis. *Int J Radiat Oncol Biol Phys* 1994;28: 797–802.
3. Uematsu M, Shioda A, Tahara K, *et al.* Focal, high dose, and fractionated modified stereotactic radiation therapy for lung carcinoma patients: A preliminary experience. *Cancer* 1998; 82:1062–1070.
4. Uematsu M, Shioda A, Suda A, *et al.* Computed tomography-guided frameless stereotactic radiotherapy for stage I non-small cell lung cancer: A 5-year experience. *Int J Radiat Oncol Biol Phys* 2001;51:666–670.
5. Takeda T, Takeda A, Kunieda E, *et al.* Radiation injury after hypofractionated stereotactic radiotherapy for peripheral small lung tumors: Serial changes in CT. *AJR* 2004;182:1123–1128.
6. Onimaru R, Shirato H, Shimizu S, *et al.* Tolerance of organs at risk in small-volume, hypofractionated, image-guided radiotherapy for primary and metastatic lung cancers. *Int J Radiat Oncol Biol Phys* 2003;56:126–135.
7. Trotti A, Byhardt R, Stetz J, *et al.* Common toxicity criteria: Version 2.0. An improved reference for grading the acute effects of cancer treatment: Impact on radiotherapy. *Int J Radiat Oncol Biol Phys* 2000;47:13–47.
8. Takizawa T, Haga M, Yagi N, *et al.* Pulmonary function after segmentectomy for small peripheral carcinoma of the lung. *J Thorac Cardiovasc Surg* 1999;118:536–541.
9. Bolliger CT, Jordan P, Soler M, *et al.* Pulmonary function and exercise capacity after lung resection. *Eur Respir J* 1996;9: 415–421.
10. Kaseda S, Aoki T, Hangai N, *et al.* Better pulmonary function and prognosis with video-associated thoracic surgery than with thoracotomy. *Ann Thorac Surg* 2000;70:1644–1646.
11. Wernly JA, De Meester TR, Kirchner PT, *et al.* Clinical value of quantitative ventilation-perfusion lung scans in the surgical management of bronchogenic carcinom. *J Thorac Cardiovasc Surg* 1980;80:535–543.
12. Bria WF, Kanarek DJ, Kazemi H, *et al.* Prediction of postoperative pulmonary function following thoracic operations. Value of ventilation-perfusion scanning. *J Thorac Cardiovasc Surg* 1983;86:186–192.
13. Kwa SLS, Lebesque JV, Theuws JCM, *et al.* Radiation pneumonitis as a function of mean lung dose: An analysis of pooled data of 540 patients. *Int J Radiat Oncol Biol Phys* 1998;42: 1–9.
14. Sunyach MP, Falchero L, Pommer P, *et al.* Prospective evaluation of early lung toxicity following three-dimensional conformal radiation therapy in non-small-cell lung cancer: Preliminary results. *Int J Radiat Oncol Biol Phys* 2000;48:459–463.
15. Abratt RP, Wilcox PA. The effect of irradiation on lung function, and perfusion in patients with lung cancer. *Int J Radiat Oncol Biol Phys* 1995;31:915–919.
16. Sansores RH, Pare P, Abbound RT, *et al.* Effect of smoking cessation on pulmonary carbon monoxide diffusing capacity and capillary blood volume. *Am Rev Respir Dis* 1992;146: 959–964.
17. Graham MV, Purdy JA, Emami B, *et al.* Clinical dose-volume histogram analysis for pneumonitis after 3D treatment for non-small cell lung cancer (NSCLC). *Int J Radiat Oncol Biol Phys* 1999;45:323–329.
18. Tsujino K, Hirota S, Endo M, *et al.* Predictive value of dose-volume histogram parameters for predicting radiation pneumonitis after concurrent chemoradiation for lung cancer. *Int J Radiat Oncol Biol Phys* 2003;55:110–115.

ELSEVIER

Int. J. Radiation Oncology Biol. Phys., Vol. 61, No. 4, pp. 1117–1122, 2005

0360-3016/05/$–see front matter

doi:10.1016/j.ijrobp.2004.07.692

CLINICAL INVESTIGATION — Lung

A PHASE II STUDY OF HYPERFRACTIONATED ACCELERATED RADIOTHERAPY (HART) AFTER INDUCTION CISPLATIN (CDDP) AND VINORELBINE (VNR) FOR STAGE III NON-SMALL-CELL LUNG CANCER (NSCLC)

SATOSHI ISHIKURA, M.D.,* YUICHIRO OHE, M.D.,† KEIJI NIHEI, M.D.,* KAORU KUBOTA, M.D.,† RYUTARO KAKINUMA, M.D.,† HIRONOBU OHMATSU, M.D.,† KOICHI GOTO, M.D.,† SEIJI NIHO, M.D.,† YUTAKA NISHIWAKI, M.D.,† AND TAKASHI OGINO, M.D.*

*Divisions of Radiation Oncology and †Thoracic Oncology, National Cancer Center Hospital East, Kashiwa, Chiba, Japan

Purpose: The purpose was to assess the feasibility and efficacy of hyperfractionated accelerated radiotherapy (HART) after induction chemotherapy for Stage III non-small-cell lung cancer.
Methods and Materials: Treatment consisted of 2 cycles of cisplatin 80 mg/m² on Day 1 and vinorelbine 25 mg/m² on Days 1 and 8 every 3 weeks followed by HART, 3 times a day (1.5, 1.8, 1.5 Gy, 4-h interval) for a total dose of 57.6 Gy.
Results: Thirty patients were eligible. Their median age was 64 years (range, 46–73 years), 24 were male, 6 were female, 8 had performance status (PS) 0, 22 had PS 1, 9 had Stage IIIA, and 21 had Stage IIIB. All but 1 patient completed the treatment. Common grade ≥3 toxicities during the treatment included neutropenia, 25; infection, 5; esophagitis, 5; and radiation pneumonitis, 3. The overall response rate was 83%. The median survival was 24 months (95% confidence interval [CI], 13–34 months), and the 2-year overall survival was 50% (95% CI, 32–68%). The median progression-free survival was 10 months (95% CI, 8–20 months).
Conclusion: Hyperfractionated accelerated radiotherapy after induction of cisplatin and vinorelbine was feasible and promising. Future investigation employing dose-intensified radiotherapy in combination with chemotherapy is needed. © 2005 Elsevier Inc.

Non-small-cell lung cancer, Hyperfractionated accelerated radiation therapy, Chemoradiotherapy.

INTRODUCTION

Lung cancer is the leading cause of cancer-related death for men and the second for women in Japan. During 2001, approximately 55,000 patients died of lung and bronchus cancer (1). Surgery is the standard of care for patients with Stage I–II non-small-cell lung cancer (NSCLC), but a combination of chemotherapy and thoracic radiotherapy with or without surgery is indicated for the majority of patients with Stage III disease. Cisplatin (CDDP) based chemotherapy with conventional radiotherapy improved survival compared to conventional radiotherapy alone (2–6) and was the standard of care in the 1990s. Recently, concurrent chemoradiotherapy has been revealed to be superior to sequential chemoradiotherapy (7, 8), but it is difficult to give full-dose chemotherapy using newer cytotoxic agents concurrently with radiotherapy, and the optimal combination has not yet been clarified. In the meantime, continuous hyperfractionated accelerated radiotherapy (CHART) with 3 daily fractions to intensify the local effect of radiotherapy has been found to be superior to conventional radiotherapy (9). The survival benefit of CHART was encouraging, but the protocol including treatments on weekends and 6-h intervals between fractions had some difficulties in practicality. Mehta *et al.* introduced hyperfractionated accelerated radiotherapy (HART) (modified CHART) with 3 daily fractions and 4-h interfraction intervals with weekend breaks and also showed promising results similar to those using sequential chemoradiotherapy (10). After these results, we started a Phase II trial to evaluate the feasibility and efficacy of induction chemotherapy with HART for patients with Stage III NSCLC.

METHODS AND MATERIALS

Eligibility criteria

Eligibility criteria included previously untreated patients with pathologically proven NSCLC with clinical tumor-node-metastasis system Stage III, and pathologic N2 was also required for Stage

Reprint requests to: Satoshi Ishikura, M.D., Radiation Oncology Division, National Cancer Center Hospital East, 6-5-1 Kashiwanoha, Kashiwa 277-8577, Japan. Tel: (+81) 4-7133-1111; Fax: (+81) 4-7131-4724; E-mail: sishikur@east.ncc.go.jp

This study was presented in part at the 38th Annual Meeting of ASCO in Orlando, Florida, May 18–21, 2002.

Acknowledgment—We thank Mrs. Fumiko Ko for her contribution to data management.

Received Mar 29, 2004, and in revised form Jul 9, 2004. Accepted for publication Jul 13, 2004.

IIIA; age, 20 to 74 years; performance status (PS) (based on Eastern Cooperative Oncology Group [ECOG] scale) 0 to 1; measurable disease; adequate hematologic (WBC count ≥4,000/mm^3, platelet count ≥100,000/mm^3, and hemoglobin ≥9.5 g/dL), hepatic (AST and ALT level ≤2 times the upper limit of normal and total bilirubin level ≤ the upper limit of normal), and renal (creatinine ≤1.2 mg/dL and creatinine clearance ≥60 mL/min) functions; PaO_2 ≥70 torr; no pleural and pericardial effusion; radiation field encompassed one-half or less of the ipsilateral lung; and no serious comorbidity. All patients signed written informed consent in accordance with our institutional review board.

Pretreatment evaluation included history and physical examination; serum chemistries (lactate dehydrogenase, alkaline phosphatase, AST, ALT, bilirubin, albumin, creatinine, and calcium); chest radiograph; CT scan of the chest; ultrasound of the abdomen; MRI or CT scan of the brain; and bone scintigraphy.

Treatment details

The treatment consisted of 2 cycles of CDDP 80 mg/m^2 on Day 1 and vinorelbine (VNR) 25 mg/m^2 on Days 1 and 8 every 3 weeks followed by HART; 3 times a day with minimal interval of 4 hours for a total dose of 57.6 Gy in 36 fractions over 2.5 weeks.

Radiation therapy was started after the patient recovered from the toxicity of chemotherapy and was delivered with megavoltage equipment. Lung heterogeneity corrections were not used. The first and third fraction of each day consisted of anterior-posterior opposed fields that encompassed the primary tumor, the metastatic lymph nodes, and the regional lymph nodes with a 1.5 to 2-cm margin. The fraction size was 1.5 Gy. Regional nodes excluding the contralateral hilar and supraclavicular nodes were included in these fractions. However, lower mediastinal nodes were included only if the primary tumor was located in the lower lobe of the lung. The second fraction of each day consisted of bilateral oblique fields that encompassed the primary tumor and the metastatic lymph nodes with a 1.5 to 2-cm margin; the fraction size was 1.8 Gy. Attempts were made to design the field of the second fraction to minimize the irradiated volume of the esophagus without compromising the margin around the tumor or spinal cord.

Toxicity assessment

Patients were observed weekly during treatment to monitor toxicity. Toxicity was graded according to the National Cancer Institute Common Toxicity Criteria (version 2.0). Late toxicity was graded according to the Radiation Therapy Oncology Group (RTOG)/European Organization for Research and Treatment of Cancer late radiation morbidity scoring scheme. Late toxicity was defined as that occurring more than 90 days after treatment initiation.

Follow-up evaluation

The following evaluations were performed until disease progression every 2 months for the first year, every 3 months for the second year, and every 6 months thereafter: physical examination, toxicity assessment, and chest radiograph. CT scan of the chest was performed at 1, 3, 6, 9, 12, 18, and 24 months after the treatment and when indicated thereafter. Restaging at 6 months after the treatment was also performed with ultrasound of the abdomen, MRI or CT scan of the brain, and bone scintigraphy.

Response assessment

Complete response (CR) was defined as complete disappearance of all measurable and assessable lesions for ≥4 weeks, partial response (PR) was defined as a decrease of 50% or more from baseline in the sum of products of perpendicular diameters of all measurable lesions for ≥4 weeks, and progressive disease (PD) was defined as an increase of 25% or more from baseline in the sum of products of perpendicular diameters of all measurable lesions or the appearance of any new lesion. Stable disease was defined as the remainder of evaluable patients without CR, PR, or PD.

Pattern of failure

Patterns of failure were defined as first site of failure. Local/regional failure included the primary tumor and regional lymph nodes. Distant failure included any site beyond the primary tumor and regional lymph nodes.

Statistics

A Simon's two-stage optimal design was used for this study with the assumption that a protocol compliance rate of less than 60% would not be feasible, and protocol compliance rate of 80% or greater with α error of 0.10 and β error of 0.10 would warrant further investigation of this regimen. In the first stage, 11 assessable patients were entered. If fewer than 7 patients completed the treatment, accrual would be stopped with the conclusion that the regimen was not feasible for further investigation. If 7 or more patients completed the treatment, an additional 27 patients would be accrued in the second study. According to this design, this study would be determined to be feasible and be proceeded to a multicenter Phase II study if 27 patients completed the treatment. The actuarial median survival time and 2-year survival were estimated by the Kaplan–Meier method (11).

RESULTS

Patient population

Between July 1999 and March 2001, 30 patients were enrolled in the study. The accrual was stopped, because 29 of 30 patients completed the treatment, and conclusions could be drawn at that time. The patients' median age was 64 years (range, 46–73 years), 24 were male, and 6 were female. The patient and tumor characteristics are summarized in Table 1.

Treatment compliance and toxicity

All patients completed 2 cycles of induction chemotherapy. Six of 30 patients required dose modification, and 13 patients had treatment delay. The median time to start of HART from start of chemotherapy was 49 days (range, 41–62 days). Twenty-nine of 30 patients completed HART, and the median overall treatment time of HART was 17 days (range, 16–22 days). In total, 29 of 30 patients (97%; 95% confidence interval [CI], 83–100%) completed this combined treatment.

The toxicity profile of the treatment is shown in Tables 2 and 3. Common Grade 3 or greater acute toxicities were neutropenia, 25 (83%); infection, 5 (17%); esophagitis, 5 (17%); and radiation pneumonitis, 3 (19%). There were 2 cases of treatment-related death due to radiation pneumonitis. As of the date of this analysis, 2 cases with Grade

Table 1. Patient and tumor characteristics

Number of patients	30
Age	
Median	64
Range	46–73
Gender	
Male	24
Female	6
Performance status	
0	8
1	22
Weight loss	
<5%	25
≥5%	5
Tumor and lymph nodes	
T1N2	3
T1N3	1
T2N2	5
T2N3	5
T3N2	1
T4N0	1
T4N1	4
T4N2	9
T4N3	1
Stage	
IIIA	9
IIIB	21
Histology	
Squamous	13
Nonsquamous	17

3 s.c. tissue fibrosis and 1 case with spontaneous rib fracture were observed as late toxicities.

Response and survival

Of 30 patients, 2 achieved CR, and 23 achieved PR with a response rate of 83% (95% CI, 65–94%). Five patients remained in a stable disease state, and there were no PD patients. With a median follow-up period of 40 months for surviving patients, the median survival and the 2-year and 3-year survivals (Fig. 1) were 24 months (95% CI, 13–34 months), 50% (95% CI, 32–68%), and 32% (95% CI, 15–49%), respectively. The median progression-free survival and the 1-year progression-free survival (Fig. 2) were 10 months (95% CI, 8–20 months) and 47% (95% CI, 29–65%), respectively.

Pattern of failure

At the time of this analysis, 22 of 30 patients (73%) showed tumor progression, 2 patients (7%) had died as a result of treatment, and 6 patients (20%) were alive without disease progression. The patterns of first failure were as follows: local/regional only, 13 (43%); local/regional and distant, 4 (13%); distant only, 5 (17%).

DISCUSSION

In the 1970s, treatment of locally advanced NSCLC was by conventional radiotherapy alone. In the 1980s, sequential chemotherapy and conventional radiotherapy were revealed to be superior to conventional radiotherapy alone. In the 1990s, optimal sequences of chemoradiotherapy and radiation fractionation were investigated. The West Japan Lung Cancer Group compared sequential vs. concurrent radiotherapy with induction CDDP, vindesine, and mitomycin (7). In an RTOG 9410 trial, induction CDDP and vinblastine plus sequential standard radiotherapy, CDDP and vinblastine plus concurrent standard radiotherapy, and CDDP and etoposide plus concurrent twice-daily hyperfractionated radiotherapy were compared (8). Both trials showed similar results; concurrent chemoradiotherapy was superior to the sequential approach and achieved 5-year survivals for concurrent and sequential approach of approximately 20% and 10%, respectively. However, twice-daily hyperfractionated radiotherapy, which seemed to be promising in a preceding RTOG 9015 trial (12), failed to show a survival advantage over standard once-daily radiotherapy, and concurrent chemotherapy and once-daily radiotherapy is the standard of care today. Recently, a Czech randomized Phase II trial (13) suggested a similar advantage of the concurrent approach using CDDP and VNR, a newer cytotoxic agent. However, there remains some argument that newer cytotoxic agents cannot be delivered as full-dose chemotherapy with concurrent radiotherapy, and the survival advantage of newer cytotoxic agents over old ones has not yet been demonstrated in Stage III NSCLC patients. The optimal schedule and fractionation of thoracic radiotherapy in combination with chemotherapy also remains to be determined.

Another promising regimen was altered fractionation of radiotherapy such as CHART or HART, 3 times a day with a fraction interval of 4 to 6 hours over 2.5 weeks or less. CHART was developed at Mount Vernon Hospital, United Kingdom, in the 1980s. It was designed to combine both a shortening of the overall treatment time of radiotherapy, which is analogous to the concept of dose intensification of cytotoxic chemotherapy, and a reduction in dose per fraction. The rationale was to overcome accelerated repopulation of the tumor during the course of radiotherapy, which may lead to local failure, and to reduce normal tissue toxicities that depend on the dose per fraction. After the results of a randomized trial that showed survival benefits of CHART over conventional

Table 2. Hematologic toxicities (n = 30)*

	Grade					
	0	1	2	3	4	≥Grade 3 (%)
Leukopenia	1	3	8	16	2	18 (60)
Neutropenia	3	0	2	6	19	25 (83)
Thrombocytopenia	20	7	1	2	0	2 (7)
Anemia	1	10	16	3	0	3 (10)

* National Cancer Institute–Common Toxicity Criteria version 2.

Table 3. Nonhematologic toxicities (n = 30)*

	Grade						
	0	1	2	3	4	5	≥Grade 3 (%)
Acute toxicity							
Nausea	7	16	4	3	0	0	3 (10)
Vomiting	23	3	4	0	0	0	0
Infection	20	3	2	5	0	0	5 (17)
Esophagitis	1	11	13	4	1	0	5 (17)
Pneumonitis	18	4	5	1	0	2	3 (10)
Late radiation morbidity†							
Esophagus	26	1	0	0	0	0	0
Heart	26	0	1	0	0	0	0
Lung	9	13	5	0	0	0	0
Subcutaneous tissue	17	6	2	2	0	0	2 (7)
Bone	26	0	0	0	1	0	1 (3)

* National Cancer Institute–Common Toxicity Criteria version 2.
† Three patients died within 90 days of the beginning of radiotherapy.

radiotherapy (9), the Department of Health in the United Kingdom recommended CHART as the radiotherapy schedule of choice in inoperable NSCLC, and a CHART implementation group was formed to facilitate its introduction throughout the United Kingdom (14). There were difficulties in changing departmental working hours and a lack of sufficient financial support in UK hospitals to introduce CHART into routine practice (15), although it was suggested that CHART gave more benefit than any sequential combination of conventional radiotherapy and chemotherapy with minimally increased toxicity. To make the accelerated regimen more widely applicable, Continuous Hyperfractionated Accelerated Radiotherapy Week-End Less (CHARTWEL) and HART were introduced and were found to be as effective as CHART. Both CHARTWEL and HART showed improved survival over conventional radiotherapy, but the local tumor control was still unsatisfactory. Radiation dose escalation and use of chemotherapy combined with CHARTWEL/HART were also investigated to improve the local control and survival. Saunders *et al.* (16) reported on CHARTWEL combined with induction chemotherapy (17). In that study, 113 patients were enrolled, and dose escalation from 54 Gy to 60 Gy with or without chemotherapy was successfully achieved. Locoregional control at 2 years was 37% and 55% for CHARTWEL 54 Gy and 60 Gy alone, respectively, compared with 72% in those treated with 60 Gy and induction chemotherapy. These results suggested that chemotherapy improved locoregional control, but unfortunately they failed to show a statistically significant survival advantage, because of the relatively small number of patients and imbalanced tumor characteristics enrolled in each arm. The advantage of dose-escalated CHARTWEL against conventional radiotherapy is currently being investigated in a German Phase

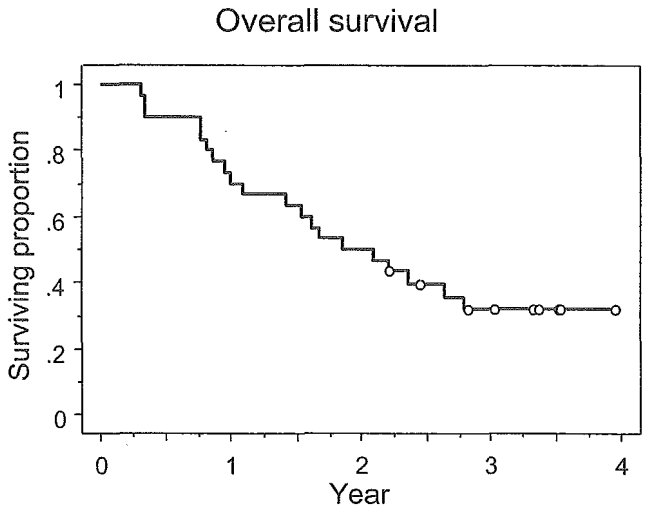

Fig. 1. Overall survival for all patients enrolled in this study.

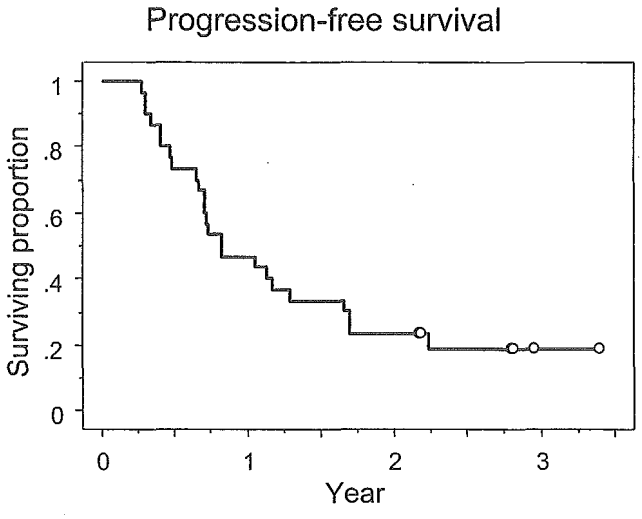

Fig. 2. Progression-free survival for all patients enrolled in this study.

III trial (18). Belani *et al.* reported the results of a randomized Phase III trial (19) that compared conventional radiotherapy with HART after induction chemotherapy (ECOG 2597). This study randomized 119 patients and unfortunately was closed because of slow accrual, but the results were provocative: The median survival time and the 2-year survivals for conventional radiotherapy and HART were 13.7 months and 33% vs. 22.2 months and 48%, respectively. These results seemed to be reliable despite the modest number of patients, because the median survival time of 13.7 months for the conventional radiotherapy arm was similar to that of a sequential chemoradiotherapy trial (2). The optimum chemotherapy regimen in combination with radiotherapy has not yet been determined, and we used a CDDP/VNR regimen instead of the carboplatin/paclitaxel regimen used in the ECOG 2597 trial. Both regimens are standards for advanced-stage NSCLC (20, 21). The compliance and toxicity profiles of chemotherapy in our study were acceptable, the incidence of esophagitis after HART was less than we expected, and the survival figure was nearly identical to that of the ECOG 2597 trial. This suggests that HART after induction CDDP/VNR or carboplatin/paclitaxel can achieve reproducible and promising results.

The pattern of failure in our study showed that local failure was still high (17 of 30, 57%) compared with distant metastasis (9 of 30, 30%), and further improvement of local control is needed. Future directions may include further dose intensification of radiotherapy and introduction of molecular-targeted agents. Recent innovation of information technology has made it possible to use sophisticated three-dimensional conformal radiotherapy (3DCRT). This can deliver intensified radiation doses to the tumor while minimizing the doses to the normal tissues that prevented further dose escalation using conventional two-dimensional radiotherapy. There have been several reports evaluating dose-intensified 3DCRT (22–25), and the technique is now under investigation in combination with cytotoxic chemotherapy in the Radiation Therapy Oncology Group trial (RTOG L-0117). Currently, molecular-targeted agents are being investigated most enthusiastically in Phase II and Phase III trials (26–29). It will be determined in the near future whether or not the combination of these agents has a survival impact. However, the optimal combination of these agents, newer cytotoxic agents, radiation fractionation, and 3DCRT will still need to be determined. Further investigation employing dose-intensified radiotherapy will be necessary to make a great leap in the treatment of locally advanced NSCLC.

REFERENCES

1. The editorial board of the cancer statistics in Japan (ed). Cancer statistics in Japan 2003. Foundation for promotion of cancer research. http://www.ncc.go.jp/en/statistics/2003/data03.pdf.
2. Dillman RO, Herndon J, Seagren SL, *et al.* Improved survival in stage III non-small-cell lung cancer: Seven-year follow-up of cancer and leukemia group B (CALGB) 8433 trial. *J Natl Cancer Inst* 1996;88:1210–1215.
3. Non-small Cell Lung Cancer Collaborative Group. Chemotherapy in non-small cell lung cancer: A meta-analysis using updated data on individual patients from 52 randomised clinical trials. *Br Med J* 1995;311:899–909.
4. Schaake-Koning C, van den Bogaert W, Dalesio O, *et al.* Effects of concomitant cisplatin and radiotherapy on inoperable non-small-cell lung cancer. *N Engl J Med* 1992;326:524–530.
5. Sause WT, Scott C, Taylor S, *et al.* Radiation Therapy Oncology Group (RTOG)88–08 and Eastern Cooperative Oncology Group (ECOG) 4588: Preliminary results of a phase III trial in regionally advanced, unresectable non-small-cell lung cancer. *J Natl Cancer Inst* 1995;87:198–205.
6. Sause W, Kolesar P, Taylor S, *et al.* Final results of phase III trial in regionally advanced unresectable non-small-cell lung cancer: Radiation Therapy Oncology Group, Eastern Cooperative Oncology Group, and Southwest Oncology Group. *Chest* 2000;117:358–364.
7. Furuse K, Fukuoka M, Kawahara M, *et al.* Phase III study of concurrent versus sequential thoracic radiotherapy in combination with mitomycin, vindesine, and cisplatin in unresectable stage III non-small-cell lung cancer. *J Clin Oncol* 1999; 17:2692–2699.
8. Curran W, Scott C, Langer C, *et al.* Long-term benefit is observed in a phase III comparison of sequential vs concurrent chemo-radiation for patients with unresected stage III NSCLC: RTOG 94–10 [Abstract]. *Proc Am Soc Clin Oncol* 2003;22:621a.
9. Saunders M, Dische S, Barrett A, *et al.* Continuous, hyperfractionated, accelerated radiotherapy (CHART) versus conventional radiotherapy in non-small cell lung cancer: Mature data from the randomised multicentre trial. *Radiother Oncol* 1999;52:137–148.
10. Mehta MP, Tannehill SP, Adak S, *et al.* Phase II trial of hyperfractionated accelerated radiation therapy for nonresectable non-small-cell lung cancer: Results of Eastern Cooperative Oncology Group 4593. *J Clin Oncol* 1998;16:3518–3523.
11. Kaplan EL, Meier P. Nonparametric estimation from incomplete observations. *J Am Stat Assoc* 1958;53:457–481.
12. Byhardt RW, Scott CB, Ettinger DS, *et al.* Concurrent hyperfractionated irradiation and chemotherapy for unresectable nonsmall cell lung cancer. Results of Radiation Therapy Oncology Group 90–15. *Cancer* 1995;75:2337–2344.
13. Zemanova M, Petruzelka L, Zemanova M. Concurrent versus sequential radiochemotherapy with vinorelbine plus cisplatin (V-P) in locally advanced non-small cell lung cancer. A randomized phase II study [Abstract]. *Proc Am Soc Clin Oncol* 2002;21:290a.
14. Macbeth F. An uncharted country. *Clin Oncol (R Coll Radiol)* 1999;11:71–72.
15. Saunders MI. Programming of radiotherapy in the treatment of non-small-cell lung cancer—a way to advance care. *Lancet Oncol* 2001;2:401–408.
16. Saunders MI, Rojas A, Lyn BE, *et al.* Dose-escalation with CHARTWEL (Continuous Hyperfractionated Accelerated Radiotherapy Week-End Less) combined with neo-adjuvant chemotherapy in the treatment of locally advanced non-small cell lung cancer. *Clin Oncol* 2002;14:352–360.
17. Bentzen SM, Saunders MI, Dische S. From CHART to

CHARTWEL in non-small cell lung cancer: Clinical radiobiological modelling of the expected change in outcome. *Clin Oncol* 2002;14:372–381.
18. Baumann M, Herrmann T, Matthiessen W, *et al.* CHART-WEL-Bronchus (ARO 97–1): A randomized multicenter trial to compare conventional fractionated radiotherapy with CHARTWEL radiotherapy in inoperable non-small-cell bronchial carcinoma. *Strahlenther Onkol* 1997;173:663–667.
19. Belani CP, Wang W, Johnson DH, *et al.* Induction chemotherapy followed by standard thoracic radiotherapy (Std. TRT) vs. hyperfractionated accelerated radiotherapy (HART) for patients with unresectable stage IIIA & B non-small cell lung cancer (NSCLC): Phase III study of the Eastern Cooperative Oncology Group (ECOG 2597) [Abstract]. *Proc Am Soc Clin Oncol* 2003;22:622a.
20. Kelly K, Crowley J, Bunn PA, *et al.* Randomized phase III trial of paclitaxel plus carboplatin versus vinorelbine plus cisplatin in the treatment of patients with advanced non-small-cell lung cancer: A Southwest Oncology Group Trial. *J Clin Oncol* 2001;19:3210–3218.
21. Pfister DG, Johnson DH, Azzoli CG, *et al.* American Society of Clinical Oncology treatment of unresectable non–small-cell lung cancer guideline: Update 2003. *J Clin Oncol* 2004;22:330–353.
22. Graham MV, Winter K, Purdy JA, *et al.* Preliminary results of a Radiation Therapy Oncology Group trial (RTOG 9311), a dose escalation study using 3D conformal radiation therapy in patients with inoperable nonsmall cell lung cancer [Abstract]. *Int J Radiat Oncol Biol Phys* 2001;51:20S.
23. Rosenzweig KE, Sim SE, Mychalczak B, *et al.* Elective nodal irradiation in the treatment of non-small-cell lung cancer with three-dimensional conformal radiation therapy. *Int J Radiat Oncol Biol Phys* 2001;50:681–685.
24. Hayman JA, Martel MK, Ten Haken RK, *et al.* Dose escalation in non–small-cell lung cancer using three-dimensional conformal radiation therapy: Update of a phase I trial. *J Clin Oncol* 2001;19:127–136.
25. Thirion P, Mc Gibney C, Holmberg O, *et al.* 3-dimensional conformal radiation therapy (3DCRT) permits radiobiological dose escalation for non-small-cell lung cancer (NSCLC): Preliminary results of a phase I/II trial [Abstract]. *Proc Am Soc Clin Oncol* 2001;20:344a.
26. Gandara DR, Chansky K, Albain KS, *et al.* Consolidation docetaxel after concurrent chemoradiotherapy in stage IIIB non-small-cell lung cancer: Phase II Southwest Oncology Group Study S9504. *J Clin Oncol* 2003;21:2004–2010.
27. Milas L, Fan Z, Andratschke NH, *et al.* Epidermal growth factor receptor and tumor response to radiation: In vivo preclinical studies. *Int J Radiat Oncol Biol Phys* 2004;58:966–971.
28. Ochs JS. Rationale and clinical basis for combining gefitinib (IRESSA, ZD1839) with radiation therapy for solid tumors. *Int J Radiat Oncol Biol Phys* 2004;58:941–949.
29. Choy H, Milas L. Enhancing radiotherapy with cyclooxygenase-2 enzyme inhibitors: A rational advance? *J Natl Cancer Inst* 2003;95:1440–1452.

Int. J. Radiation Oncology Biol. Phys., Vol. 64, No. 4, pp. 1229–1236, 2006

0360-3016/06/$–see front matter

ELSEVIER

doi:10.1016/j.ijrobp.2005.11.016

PHYSICS CONTRIBUTION

SPEED AND AMPLITUDE OF LUNG TUMOR MOTION PRECISELY DETECTED IN FOUR-DIMENSIONAL SETUP AND IN REAL-TIME TUMOR-TRACKING RADIOTHERAPY

HIROKI SHIRATO, M.D.,* KEISHIRO SUZUKI, M.D.,* GREGORY C. SHARP, PH.D.,†
KATSUHISA FUJITA, R.T.,* RIKIYA ONIMARU, M.D.,* MASAHARU FUJINO, M.D.,* NORIO KATO, M.D.,*
YASUHIRO OSAKA, M.D.,* RUMIKO KINOSHITA, M.D.,* HIROSHI TAGUCHI, M.D.,*
SHUNSUKE ONODERA, M.D.,* AND KAZUO MIYASAKA, M.D.*

*Department of Radiology, Hokkaido University School of Medicine, Sapporo, Japan; †Department of Radiation Oncology, Massachusetts General Hospital, Harvard Medical School, Boston, MA

Background: To reduce the uncertainty of registration for lung tumors, we have developed a four-dimensional (4D) setup system using a real-time tumor-tracking radiotherapy system.
Methods and Materials: During treatment planning and daily setup in the treatment room, the trajectory of the internal fiducial marker was recorded for 1 to 2 min at the rate of 30 times per second by the real-time tumor-tracking radiotherapy system. To maximize gating efficiency, the patient's position on the treatment couch was adjusted using the 4D setup system with fine on-line remote control of the treatment couch.
Results: The trajectory of the marker detected in the 4D setup system was well visualized and used for daily setup. Various degrees of interfractional and intrafractional changes in the absolute amplitude and speed of the internal marker were detected. Readjustments were necessary during each treatment session, prompted by baseline shifting of the tumor position.
Conclusion: The 4D setup system was shown to be useful for reducing the uncertainty of tumor motion and for increasing the efficiency of gated irradiation. Considering the interfractional and intrafractional changes in speed and amplitude detected in this study, intercepting radiotherapy is the safe and cost-effective method for 4D radiotherapy using real-time tracking technology. © 2006 Elsevier Inc.

Four-dimensional radiotherapy, Setup, Real-time tracking, Four-dimensional setup.

INTRODUCTION

Four-dimensional (4D) radiotherapy, a concept to increase the accuracy of localization in space as well as in time by accounting for spatiotemporal changes in the anatomy during radiotherapy, has been receiving more and more attention (1). Four-dimensional treatment planning is increasingly used to reduce the uncertainty resulting from organ motion of computed tomography (CT) (1–3). Second, a therapeutic beam is delivered to the moving tumor by real-time tumor-tracking technology in which a gated beam intercepts the tumor trajectory (4) or in which the tumor position is pursued dynamically (5). Third, verification of the tumor position during irradiation is required for quality assurance (6). Each step in 4D radiotherapy (4DRT) is quite important. One of the most important steps is the accurate registration of the tumor position at the same phase of internal tumor motion as in the treatment planning. Without this, we will miss the tumor in 4DRT.

To our knowledge, no 4D setup method—that is, a method for setting up tumors in motion at the right time and with the right coordinates—has been reported. We have developed a 4D setup system using a fluoroscopic real-time tumor-tracking radiotherapy (RTRT) system (1, 4). In this paper, we describe our approach to performing 4D setup using the RTRT system. We describe also what we have found about interfractional and intrafractional changes in the amplitude and speed of internal tumor motion using the 4D setup system.

METHODS AND MATERIALS

Four-dimensional setup

The RTRT system has been already described in detail (1, 4). In brief, three 1.5-mm fiducial markers are implanted near a lung tumor through bronchial fiberscopy. Two sets of fluoroscopy in the treatment room are used to detect the three-dimensional (3D) coordinates of each internal fiducial marker. The distances be-

Reprint requests to: Hiroki Shirato, Department of Radiology, Hokkaido University School of Medicine, North-15 West-7, Sapporo 060-8636, Japan. Tel: (+81) 11-706-7876; Fax: (+81) 11-706-5975; E-mail: hshirato@radi.med.hokudai.ac.jp

Received Aug 5, 2005, and in revised form Nov 8, 2005. Accepted for publication Nov 17, 2005.

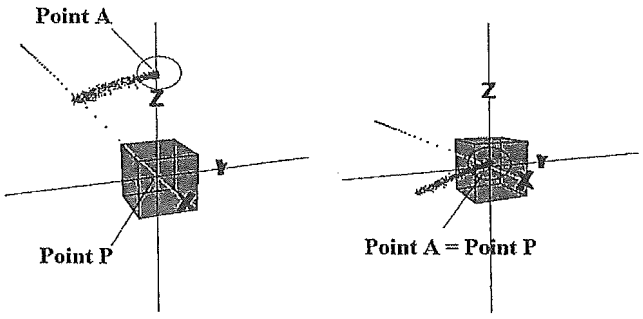

(a) Before 4D setup (b) After 4D setup

Fig. 1. Trajectory of a marker near a lung tumor in a patient with lung cancer before and after four-dimensional setup. Each spot corresponds to the position of the marker as detected by the real-time tumor-tracking radiotherapy system. In this case, Point P and the gating window (box) were set at the isocenter with 2 mm isotropical "permitted dislocation" from Point P. The actual position of the marker at the end of expiration, Point A, in the trajectory of the marker is adjusted to Point P by moving the treatment couch. The *x*, *y*, and *z* are consistent with the right-left, craniocaudal, and anteroposterior directions, respectively.

tween markers are measured to rule out the possibility of the migration of the markers. The 3D coordinates of the marker that is closest to the tumor are automatically detected 30 times per second by using a real-time pattern-recognition algorithm in which image processors compare the digitized image and the template image of a metallic marker to detect the location of the marker (6). The coordinates of the center of the gold marker were determined using a 16 × 16 pixel image template of the marker. The accuracy of the measurement was estimated to be 0.5 ± 0.2 mm in phantom experiments (4).

In our protocol for lung cancer using the 4D setup, the following steps are involved.

1. After the insertion of the fiducial markers, a multidetector CT is taken as the patient holds his or her breath at the end of expiration, where a previous study of ours found that gating efficiency is highest (7). Transaxial reconstructed CT with a slice thickness of 1 mm is used for treatment planning. Three-dimensional conformal radiotherapy is planned on a 3D radiation treatment planning system. The fiducial marker is contoured on the 3D radiation treatment planning system, and its coordinates relative to the isocenter are transferred to the 4D setup system in the RTRT system. The planned coordinates of the fiducial marker relative to the isocenter are visually demonstrated in a room's-eye view on a display of the 4D setup system as Point P in Fig. 1. The *x*, *y*, and *z* axes correspond to the right-left (RL), craniocaudal (CC), and anteroposterior (AP) directions, respectively. The size of the gating window around Point P can be determined anisotropically in the RL, CC, and AP directions and visualized as a box in the room's-eye view on the display (Fig. 1). In our protocol for lung tumors, the gating window is selected to be isotropic ±2.0 mm for the RL, CC, and AP directions.
2. The RTRT system records the coordinates of the internal fiducial marker for 1 to 2 min at the rate of 30 times per second before the start of treatment. The recorded 3D coordinates of the internal marker are visually demonstrated as the trajectory of the marker in the room's-eye view on a display of the 4D setup system (Fig. 1). Each spot in Fig. 1 corresponds to the coordinates of the marker as detected by the RTRT system 30 times per second.
3. The operator can determine which part of the trajectory is to be used for gating, as follows. One can select the actual coordinates of the marker in the trajectory (Point A). This point can be selected so as to maximize the gating efficiency according to computer guidance. The selected Point A is usually near the end of the expiration phase or near the maximum CC coordinates (the most cranial position) in the trajectory. If the selected point is not near the end of the expiration phase, one can change the position of Point A to be compatible with the point at the end of the expiration phase that was used in the CT planning.
4. In daily radiotherapy, patients are first positioned on the treatment couch with the use of skin markers and lasers in the treatment room.
5. For 1 to 2 min, the coordinates of the fiducial marker, or 3D trajectory, are recorded using the 4D setup system before daily irradiation. This trajectory usually has some interfractional deviation, so the operator needs to determine every day which part of the trajectory, or Point A, would be compatible with the trajectory in the 4D setup system recorded in Steps 1 to 4, according to computer guidance.
6. The table position is shifted by adjusting Point A in the trajectory to the planned position of the marker, Point P, which has been determined in 3D conformal radiotherapy.
7. Real-time tumor-tracking radiotherapy is started using the gating window around Point P. A therapeutic beam is delivered only when the actual position of the marker is within the gating window or within the permitted distance from Point P, as we have reported (1, 4, 6). The linac is enabled during the period that the fiducial marker is within the gating window and

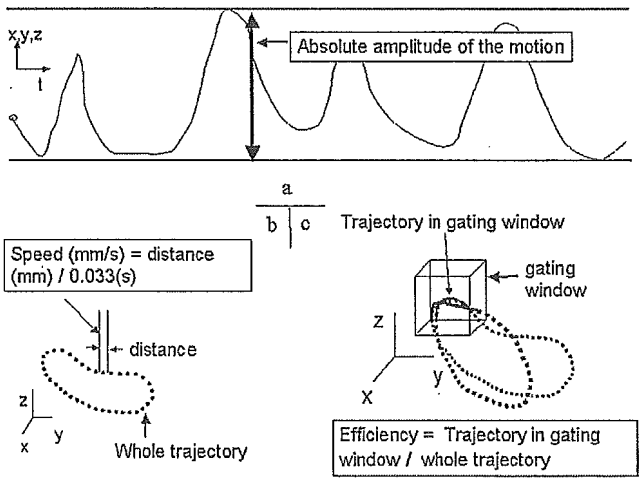

Fig. 2. (a) Absolute amplitude determined from the time signal of the tumor motion in *x*, *y*, and *z* directions. The absolute amplitudes of marker movement were defined as the distance between the maximum and minimum coordinates along each of the axes (*x*, *y*, and *z*) in each log file. (b) Speed of the marker determined from the trajectory of the marker. (c) Efficiency of irradiation determined from the trajectory of the marker and the gating window. We estimated the maximum possible efficiency achieved for each patient with a ±2 mm gating window for the right-left, craniocaudal, and anteroposterior directions.

unenabled when the marker is out of the gating window with the delay of 0.05 s.

Amplitude and speed of the tumor motion

The following study was performed using the data gathered in 21 patients in the 4D setup. The patients were treated with 1 to 8 fractions each for their peripheral lung tumors. The patients were examined with the 4D setup using the RTRT system for 5 days in 2 patients, 4 days in 7 patients, 3 days in 2, 2 days in 6, and 1 day in 4. In total, 60 treatment days, or 3 treatment days on average for each patient, were used for the analysis. The reason why 4D setup was not performed in some treatments was that the researcher was absent on that day; there was no intentional withdrawal of data.

The length of the log file for each 4D setup ranged from 60.8 to 412.1 s, with a mean of 136.4 s. The absolute amplitudes of marker movement were defined as the distance between the maximum and minimum coordinates along each of the axes (x, y, and z) in each log file (Fig. 2a). This definition of absolute amplitude is different from the definition of amplitude in our previous paper, where amplitude was determined as the parameter in a fitting curve assuming sinusoidal respiratory motion (7, 8). Variations in amplitude among patients and also among treatment days for the same patient were examined. The speed of the marker in a 3D trajectory can be determined by dividing the distance between two points by the fluoroscopic imaging pulse sequence of 1/30 s (Fig. 2b). The maximum, minimum, and median speeds of the marker in each log file were examined for each of 60 treatment days in 21 patients. Because RTRT is one type of gating irradiation, it is crucial to estimate the efficiency of therapeutic beam delivery during each treatment session. The 4D setup system can estimate the efficiency of gated irradiation at Point P at a predetermined gating window (Fig. 2c).

In this study, we estimated the maximum possible efficiency achieved for a patient with a ±2 mm gating window for the RL, CC, and AP directions. The actual treatment time using the ±2 mm gating window was recorded in 18 of the 21 patients and compared with the prediction in the 4D setup. The number of readjustments on the treatment couch needed per treatment was recorded in 6 recent patients to figure out the practical effect of baseline shifting and the importance of fine on-line remote control of the treatment couch.

RESULTS

The absolute amplitudes of the trajectories in the x, y, and z directions in 21 patients are shown in Table 1. When the 4D setup data for multiple treatments were available, the absolute amplitude was averaged. In 60 absolute amplitudes along the RL, CC, and AP directions in 21 patients, the number of average absolute amplitudes longer than 10 mm—at which length we found, in a previous study, that gating allowed a meaningful reduction in safety margins (9)—was 20 (33%) (Table 1). The standard deviation of the absolute amplitude was larger than 5 mm in 14 (23%) of 60 (Table 1).

The absolute amplitudes of the trajectories in the x, y, and z directions for 60 treatments in the 21 patients are shown in Fig. 3. When the 4D setup was used several times in the same patient, multiple spots were plotted vertically for that same patient in Fig. 3. Figure 3 shows that the absolute

Table 1. Absolute amplitude and speed of the internal fiducial marker detected in 4D setup system. Average and standard deviation are shown for patients for whom 4D setup was used at least twice. The average at "Total" was calculated as (the sum of the average of each patient)/(number of patients). The standard deviation at Total was for the average of each patient.

Patient no.	4D setup used during irradiation	Average absolute amplitude (mm)			Average speed (mm/s)		
		Right-left	Craniocaudal	Anteroposterior	Max.	Median	Min.
1	4	4.7 ± 1.2	4.7 ± 2.0	5.3 ± 2.6	11.3 ± 3.7	8.2 ± 1.1	6.6 ± 0.7
2	5	4.8 ± 0.5	4.2 ± 0.9	5.5 ± 0.8	43.6 ± 3.6	23.7 ± 0.8	16.2 ± 0.6
3	4	8.0 ± 7.2	17.3 ± 11.0	7.1 ± 2.2	24.7 ± 8.2	10.8 ± 0.4	6.2 ± 0.4
4	1	2.6	3	4.4	11.6	7.6	5
5	2	8 ± 1.6	8.4 ± 2.3	11.7 ± 0.3	36 ± 0.4	10.8 ± 2.0	10.3 ± 1.0
6	2	6.9 ± 6.1	15.1 ± 13.8	11.2 ± 0.0	28.8 ± 0.2	14.3 ± 3.2	9.3 ± 1.2
7	2	2.9 ± 1.6	4.2 ± 2.3	4.4 ± 1.7	8.3 ± 2.3	5 ± 0.2	3.9 ± 0.5
8	1	9.5	13.1	13.7	36.1	26.8	9.1
9	2	2.2 ± 4.3	10.7 ± 1.7	5.2 ± 5.2	8.5 ± 0.3	5.9 ± 0.4	4.6 ± 0.6
10	4	6.2 ± 2.5	17.8 ± 10.1	6.2 ± 2.9	11.5 ± 3.9	7.1 ± 1.4	4.8 ± 0.7
11	4	3.4 ± 0.3	3.6 ± 0.6	3.8 ± 0.3	10.2 ± 0.8	7.4 ± 0.4	6 ± 0.4
12	1	6.4	8.6	5.8	27.6	23.3	18.7
13	4	17.6 ± 9.9	28 ± 3.2	28.4 ± 6.4	54.3 ± 31.9	9.7 ± 0.4	4 ± 1.2
14	2	10.4 ± 10.1	9.9 ± 8.5	8 ± 0.4	23.6 ± 0.3	12.5 ± 0.6	6 ± 0.3
15	5	3.9 ± 1.4	5.7 ± 1.3	3.2 ± 0.7	6.6 ± 0.6	5.5 ± 0.4	4.3 ± 0.6
16	1	6	3.6	2.9	10	7.6	6.1
17	4	19.1 ± 3.7	15.9 ± 7.7	16 ± 5.5	43.6 ± 11.4	23.7 ± 0.4	16.2 ± 2.8
18	2	24.6 ± 7.5	18.3 ± 7.2	19 ± 6.6	72.6 ± 22.5	13.5 ± 8.9	7.2 ± 6.2
19	3	8.3 ± 2.6	21.4 ± 4.3	11.5 ± 3.1	11.3 ± 3.5	6.9 ± 0.5	5.1 ± 0.8
20	3	7.4 ± 0.8	2.1 ± 0.2	2.4 ± 0.8	8.3 ± 0.2	6.6 ± 0.3	5.4 ± 0.5
21	4	8 ± 1.1	8.4 ± 0.6	11.7 ± 1.5	12.6 ± 3.4	7.4 ± 3.6	4 ± 2.2
Total	60	8.2 ± 6.5	10.7 ± 8.6	8.8 ± 7.0	21.1 ± 18.9	9.9 ± 5.4	6.6 ± 3.6

Abbreviation: 4D = four-dimensional.

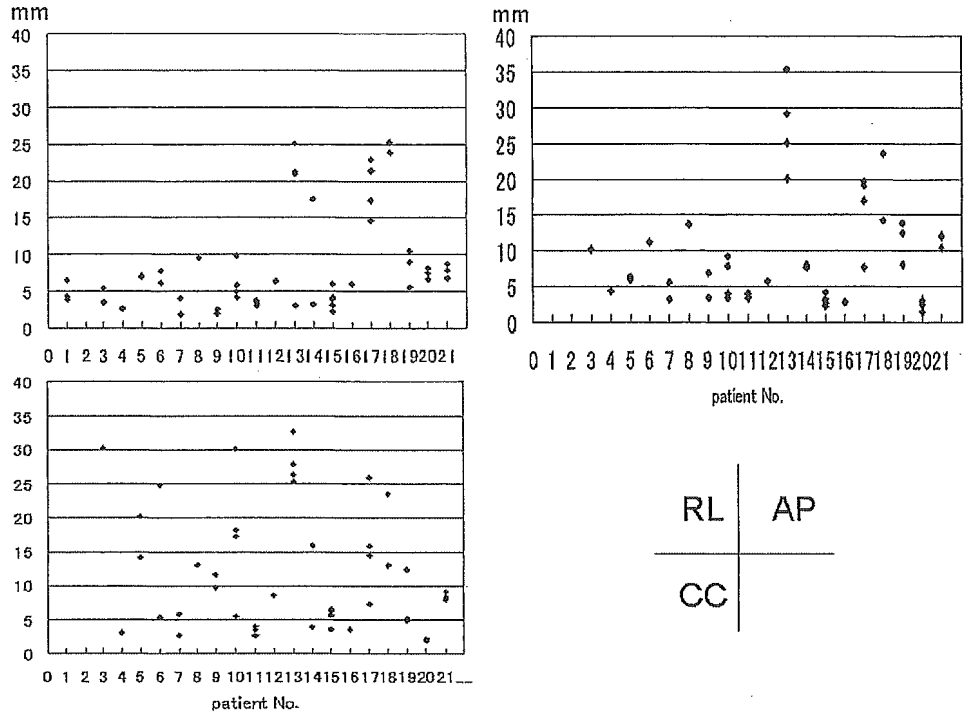

Fig. 3. The absolute amplitudes of the trajectories in right-left, craniocaudal, and anteroposterior directions for 60 treatment days in 21 patients. When the four-dimensional setup was used several times in the same patient, multiple spots were plotted vertically for that same patient. AP = anteroposterior; CC = craniocaudal; R-L = right-left.

amplitude of the marker varied considerably from patient to patient and among treatment days for the same patient. In RTRT, this variation of the absolute amplitude does not worsen the accuracy of the treatment, because the therapeutic beam is delivered only when the marker is within the gating window. However, the larger the absolute amplitude, the longer treatment time tends to be, because the size of the gating window is the same every day.

Some degree of interfractional change in the 3D trajectory of the marker was seen in all patients (Fig. 4). Figure 4 shows typical interfractional and intrafractional changes in marker trajectory from Day 1 to Day 2 in the same patient with lung cancer. It was apparent that the fluctuation of the trajectory was not simple and changed in 3D.

Figure 5 shows the 3D coordinates of the marker at the end of the exhalation and inhalation phases in one patient. The phase in a respiratory cycle was determined by assuming that the maximum and minimum y coordinates in that cycle are consistent with the end of the exhalation and inhalation phases, respectively. Intrafractional change in the coordinates at the end of the inhalation phase was apparent. In this patient, the marker positions at the end of the exhalation phase had a smaller intrafractional variation than those at the end of the inhalation phase.

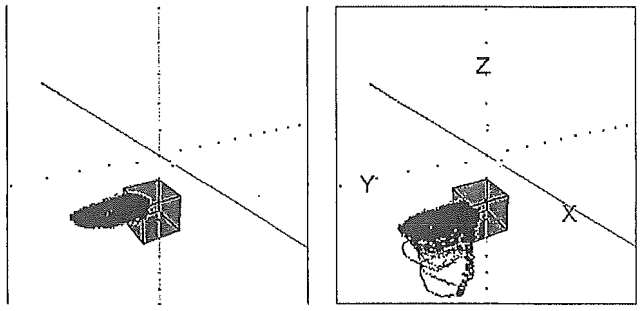

Fig. 4. Interfractional change between Days 1 and 2 in the three-dimensional trajectory of the marker in a patient with lung cancer. The gray box is the gating window. The dots are consistent with the actual positions of the internal fiducial marker detected 30 times per second.

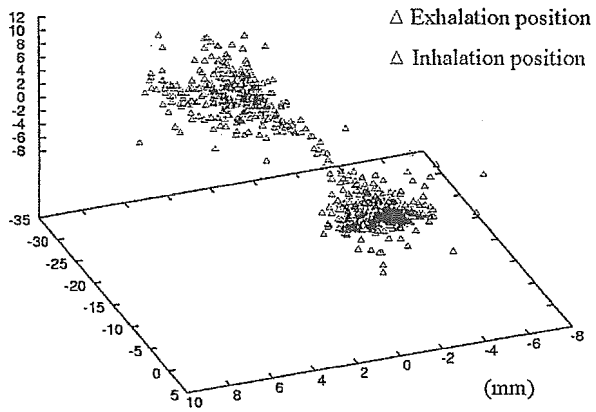

Fig. 5. Three-dimensional coordinates of the marker at the end of exhale phase (blue) and inhale phase (red) in 1 patient.

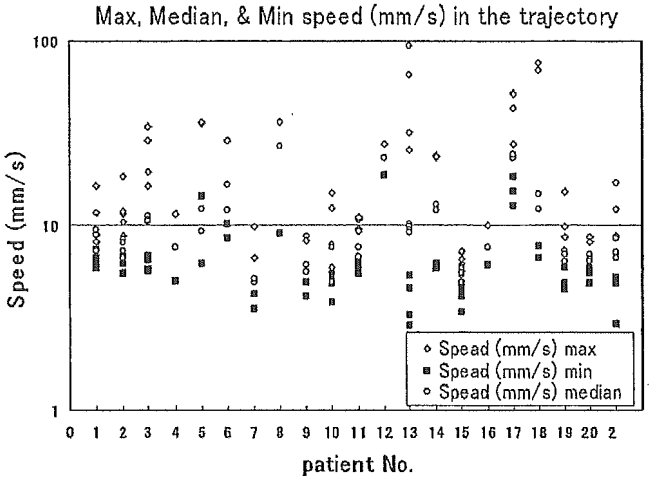

Fig. 6. The maximum, minimum, and median speeds of the marker for 60 treatment days in 21 patients are plotted in log scale.

Figure 6 shows the maximum, median, and minimum speeds of the marker (log scale) for 60 treatment days in 21 patients. It was apparent that the median speed is closer to the minimum than to the maximum speed in the majority of patients, but the median speed is close to the maximum on a few occasions. In 10 (16%) of the 60 treatments, the maximum marker speed exceeded 33 mm/s, which has been reported to be the average maximum leaf velocity at the isocenter plane of the multileaf collimator by Wijesooriya *et al.* (10). The highest average maximum speed in the present study was 94 mm/s, whereas the average maximum speed of the marker was more than 33 mm/s in 6 (29%) of 21 patients (Table 1).

Figure 7 shows the maximum efficiency of the irradiation achievable with the ±2 mm gating window for the RL, CC, and AP directions. The achievable efficiency varied considerably among patients. Even in the same patient, the achievable efficiency of the irradiation varied considerably among treatment days. Figure 8 shows how the maximum achievable efficiency changed with the size of the gating window from ±2.0, 2.5, and 3.0 mm for Point A, which is determined using 4D setup, and ±2.0, ±3.0, and ±4.0 mm for Point B,

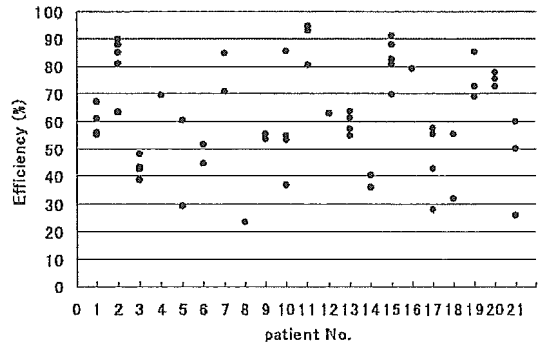

Fig. 7. The maximum efficiency of the irradiation achievable with the ±2 mm gating window for *x*, *y*, and *z* directions for 60 treatment days in 21 patients.

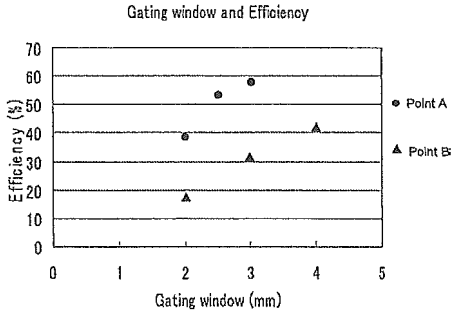

Fig. 8. The relationship between the size of the gating window and the maximum efficiency achievable in 1 patient. Point A is the maximum efficiency achievable as predicted by the four-dimensional setup system and examined at the gating window of ±2.0, ±2.5, and ±3 mm. Point B is a point arbitrarily determined by an operator without the help of the system at the gating window of ±2.0, ±3.0, and ±4.0 mm.

which is arbitrarily determined, respectively. Higher gating efficiency was predicted when we determined the Point A for gating using the 4D setup system rather than when we selected an arbitrary Point B without the help of this system. The larger gating window would be needed for Point B to achieve similar efficiency, so that normal tissue would be irradiated more when we use Point B for gating rather than Point A.

Table 2 shows the number of readjustments of the table position needed as a result of the baseline shift of the marker trajectory during RTRT in 6 patients. The achievable efficiency of the gated radiotherapy was 62.4% ± 19.0% predicted by the calculation of the 4D setup system if we used ±2 mm for the gating window. The actual treatment time was 25 ± 13 min for 10.5 ± 1.7 Gy. The actual efficiency was grossly estimated as 28% (10.5 Gy in 7 min vs. 10.5 Gy in 25 min), assuming a dose rate of 1.5 Gy/min, the most frequent rate of the linear accelerator in gating mode. The number of readjustments needed during irradiation as a result of a baseline shift of the tumor position in most patients was 4.1 ± 4.1 times per treatment day. One patient needed 21 readjustments on his initial treatment day, because he had difficulty resting quietly on the treatment couch.

DISCUSSION

Engelsman *et al.* assessed the impact of both setup errors and respiration motion on the cumulative dose delivered to a clinical target volume in the lung and found that systematic setup errors have a dominant effect on the cumulative dose to the clinical target volume; random setup errors and breathing motion have smaller effects (9). Accordingly, they recommended minimizing systematic setup errors for lung tumors in motion. Bony landmarks have been used as surrogates for the setup of the lung tumor by comparing megavoltage portal images with simulation film or digitally reconstructed radiographs (11). Reports using CT simula-

Table 2. Number of treatments, daily dose, achievable efficiency estimated by the four-dimensional setup system, actual total treatment time, and readjustments of the treatment couch per treatment. The mean total treatment time was calculated as (total treatment time)/(number of patients examined). The standard deviation in the "Total" row was for the mean time of each treatment. The number in the column "Readjustments per treatment" is the number of readjustments per treatment day including the initial setup. Each number corresponds to the number of required readjustments on the 1st, 2nd, 3rd, and 4th treatment days from left to right.

Patient no.	Number of treatments	Daily dose (Gy)	Achievable efficiency (%)	Total treatment time (minutes)	Readjustments per treatment (including one setup time)
1	4	10	59.7	35 ± 27	–*
2	8	6	81.4	—	–*
3	4	12	43.1	36 ± 8	–*
4	4	10	69.4	10 ± 1	–*
5	4	12	44.9	34 ± 13	–*
6	4	12	48.1	23 ± 4	–*
7	4	10	77.8	12 ± 1	–*
8	4	10	23.5	17 ± 3	–*
9	4	10	44.1	14 ± 1	–*
10	4	10	57.6	19 ± 3	–*
11	4	10	90.4	9 ± 1	–*
12	1	15	62.9	—	–*
13	4	10	59.2	—	–*
14	4	10	38.3	28 ± 7	–*
15	4	12	82.4	17 ± 0	–*
16	4	10	79.1	15 ± 4	2, 3, 3, 2
17	4	10	45.9	28 ± 3	21, 6, 3, 2
18	4	10	43.7	31 ± 5	4, 5, 3, 2
19	4	12	75.7	17 ± 2	2, 2, 5, 2
20	4	10	75.3	21 ± 4	2, 3, 3, 2
21	4	10	48.9	41 ± 18	5, 5, 2, 10
Total	85	10.5 ± 1.7	62.4 ± 19.0	25 ± 13	4.1 ± 4.1

* No data available.

tion did, however, raise questions about the reliability of bony landmarks for the positioning of lung tumors (12, 13).

The present findings showed that the variation of the absolute amplitude of the trajectory among patients was remarkable not only in the craniocaudal direction but also in the lateral and anterodorsal directions. Four-dimensional planning using CT images at different respiratory phases, or usage of 4DCT, has been useful for determining the different internal target volumes for individual patients, incorporating changes in the position and shape of the tumor (14–17). These techniques are useful for assessing the magnitude of respiratory motion, to the extent that the motion is reproducible or negligible. However, we have found that the magnitudes of the interfractional and intrafractional changes in the same patient were often remarkable in terms of absolute amplitude. The variation was large not only in the CC direction but also in the RL and AP directions. Our study suggests that, in planning with 4DCT, it is important to estimate the residual uncertainty of tumor motion with respect to its interfractional and intrafractional changes.

To reduce interfractional and intrafractional errors due to variation in the motion of the tumor, real-time tracking technology is now expected to be useful and practical. In the use of real-time tracking technology in radiotherapy, two concepts have been reported. One is *intercepting radiotherapy,* in which a therapeutic beam is gated to irradiate a tumor at a planned position by intercepting the trajectory of the tumor motion. This has been used for lung tumors with the RTRT system developed at our institution. The shortcoming of the intercepting radiotherapy is lower efficiency than conventional nongated radiotherapy. The present study showed that even with a table shift, the achievable gating efficiency is only 62.4% ± 19%, which has room for improvement. The other method reported is *pursuing radiotherapy,* in which the position of the tumor is monitored using real-time tracking technology, and the moving aperture of a linear accelerator is synchronized with the tumor's motion to irradiate the tumor continuously (5, 18, 19). The latter method is expected to increase efficiency and decrease treatment time. Precise prediction of tumor motion is expected to be useful to decrease treatment time (20). Previous data have been predicted well with some mathematical models (21, 22). However, the present study showed that the speed of the tumor varied considerably during a single treatment session and among treatment days in the same patient. Some patients' tumors move as fast as 90 mm/s, so mechanical control of the aperture for pursing radiotherapy may be difficult without some cutoff level for the speed to follow, as Wijesooriya *et al.* reported (10). Interestingly enough, the present study showed that the variation in median and minimum speeds was not as large as that in median and maximum speeds (Table 2). This finding is